Published in final edited form as:
Bioorg Med Chem. 2009 February 15; 17(4): 1486–1493. doi:10.1016/j.bmc.2009.01.014.

^{64}Cu-AMD3100 - A novel imaging agent for targeting chemokine receptor CXCR4

Orit Jacobson[1], **Ido D. Weiss**[2], **Lawrence Szajek**[3], **Joshua Farber**[2], and **Dale O. Kiesewetter**[1]

[1] Positron Emission Tomography Radiochemistry Group, National Institute of Biomedical Imaging and Bioengineering, Bethesda, MD 20892, USA

[2] Laboratory of Molecular Immunology, National Institute of Allergy and Infectious Diseases, Bethesda, MD 20892, USA

[3] Positron Emission Tomography Department, Warren Grant Magnuson Clinical Center; National Institutes of Health, Bethesda, MD 20892, USA

Abstract

CXCR4 is a chemokine receptor which has been shown to be exploited by various tumors for increased survival, invasion, and homing to target organs. We developed a one step radiosynthesis for labeling the CXCR4-specific antagonist AMD3100 with Cu-64 to produce **^{64}Cu-AMD3100** with a specific activity of 11.28 Ci/μmol (417 GBq/μmol) at the end of radiosynthesis. Incorporation of Cu(II) ion into AMD3100 did not change its ability to inhibit cellular migration in response to the (only) CXCR4 ligand, SDF-1/CXCL12. **^{64}Cu-AMD3100** binding affinity to CXCR4 was found to be 62.7 μM. Biodistribution of **^{64}Cu-AMD3100** showed accumulation in CXCR4-expressing organs and tissues, a renal clearance pathway, and an anomalous specific accumulation in the liver. We conclude that **^{64}Cu-AMD3100** exhibits promise as a potential PET imaging agent for visualization of CXCR4-positive tumors and metastases and might be used to guide and monitor anti-CXCR4 tumor therapy.

Keywords

AMD3100; CXCR4; PET; copper-64

Introduction

Chemokines are small (8–14 kDa), mostly basic, structurally related peptides, that serve as chemotactic factors to guide migratory cells within an organism. [1] Chemokines mediate their effects through a subfamily of seven transmembrane domain, G protein-coupled receptors. The ability of chemokines to control cell trafficking is essential in various physiological processes. [2–7] More than forty chemokines [3–7] and nineteen chemokine receptors (CKRs) have been identified in humans. Chemokines play an essential role in the recruitment and activation of cells of the immune system [3]. In addition, there is strong evidence that tumor-derived chemokines are responsible for recruitment of host cells that support tumor progression, [8, 9] and CKRs were also shown to be involved in various tumor processes and metastasis. [10]

CXCR4 was originally discovered as the putative co-receptor for entry of T-tropic, but not M-tropic, strains of HIV-1 viruses into $CD4^+$ T cells; [11, 12] and extensive research has elucidated the functions of this receptor. CXCR4 has been highly conserved during evolution and can be detected in a diverse range of cells, including peripheral blood lymphocytes and monocytes, mast cells, adult $CD34^+$ bone marrow progenitor cells, endothelial cells, intestinal and alveolar epithelial cells, astrocytes, microglia, and neurons. [11, 13–17]

The native ligand for CXCR4 is the chemokine stromal cell-derived factor-1 (SDF-1), also known as CXCL12. Like CXCR4, SDF-1 has been highly conserved during evolution. SDF-1 is expressed constitutively in a number of tissues including liver, lungs, lymph nodes, adrenal glands and bone marrow. Together, the SDF-1/CXCR4 ligand-receptor pair constitutes an axis that has been shown to be involved in directing cells to organ sites with high levels of SDF-1 expression, suggesting that this interaction plays a key role in the chemotaxis, retention, and homing of hematopoietic cells during homeostasis, and in the process of cancer metastases. [18, 19] In addition, the CXCR4/SDF-1 axis plays a fundamental role in the migration of progenitor cells during embryonic development of the cardiovascular, hemopoietic, and central nervous systems, [20–24] as revealed through studies of both CXCR4 and SDF-1 knockout mice. [24–26] On the other hand, CXCR4 and SDF-1 axis have also been shown, as noted above, to be exploited by HIV infection and to have roles in other disease processes such as cancer cell metastasis, leukemia progression, rheumatoid arthritis and pulmonary fibrosis. [27–31, 10]

More than twenty-three different human tumors, including breast, prostate, lung, ovarian, pancreatic, esophageal, colorectal, and renal carcinoma, melanoma, neuroblastoma, and osteosarcoma, over-express CXCR4. [21, 22, 23, 32, 29, 9, 33] As one example of the possible importance of CXCR4 in cancer, Marchesi F. et al have shown that CXCR4 stimulates pancreatic tumor cells motility and invasion, and promotes their survival and proliferation. [34] Similarly, CXCR4 expression by tumor cells was shown to contribute to tumor growth, vascularization, and metastasis in prostate cancer xenografts in mice. [35] In accord with these data, inhibition of CXCR4 resulted in lower metastatic loads in the bones of mice injected with prostate cancer cells. [36] Up-regulation of CXCR4 has been also implicated in the pathogenesis of various neuro-degenerative and neuro-inflammatory diseases. [37–39]

CXCR4 inhibitors, both peptide-based and small molecules, have been developed as potential therapeutics. AMD3100, (Fig. 1, compound **1**), a bicyclam molecule, in which the two cyclam moieties are linked by a 1,4-phenylenebis(methylene)-bridge (Fig. 1), [40–44] has been identified as a specific inhibitor of CXCR4. AMD3100 was originally developed as an inhibitor of HIV infection that worked by blocking the interaction of viral gp120s of some strains of HIV-1 with CXCR4 on CD4 T cells, and has been shown to block HIV infection in clinical trials. Clinical trials also demonstrated that **1** is an effective mobilizer of hematopoietic stem cells from the bone marrow (BM) in both healthy individuals and some individuals with cancer, [45, 46, 47] and is likely to enter clinical practice for this indication. **1** was also found to inhibit the SDF-1-induced chemotaxis through CXCR4 by blocking migration of monocytic cells toward higher concentration of SDF-1, [48] suggesting that it might also be used to inhibit cancer metastasis.

Positron emission tomography (PET), a non-invasive molecular imaging modality, uses short-lived positron-emitting bioprobes to obtain four-dimensional, quantitative determination of the distribution of radioactivity within the body. [49, 50, 51] ^{64}Cu, ($t_{1/2}$= 12.7 h., β^+ 17.9%, electron capture 45%, β^- 37.1%), can be used for PET imaging due to its positron emission and for radiotherapy due to its electron capture and μ^- emissions in cancer treatment. [52–59]

Previous attempts to image CXCR4 for single photon emission computed tomography (SPECT) have been reported. The CXCR4 peptide antagonist Ac-TZ14011 labeled with ^{111}In, accumulated in the spleen (8% ID/g), had high accumulation in the kidneys and

liver, and displayed low accumulation in tumors (0.51% ID/g). [60] SDF-1 has been labeled with ^{99}Tc [61] and was evaluated as an imaging agent for myocardial infarction. A high dose of ^{99}Tc- SDF-1 was required to assess the accumulation in the myocardium; 0.6% ID/g accumulation was observed in the infracted myocardium compared with 0.1% ID/g in normal myocardium. [61]

In this manuscript we describe a novel radiochemical synthesis of ^{64}Cu-AMD3100 (**4**) and its evaluation as a potential imaging agent of CXCR4 expression in a living organism. We describe binding and inhibitory properties of ^{64}Cu-AMD3100 (**4**) in vitro and/or in vivo.

Material and methods

2.1 General methods

All solvents were purchased as anhydrous from Sigma-Aldrich Co. (MO, USA). ^{1}H-NMR spectra were recorded on an Avance 300 (Bruker, USA) in D_2O or $CDCl_3$. ^{1}H-NMR signals are reported in parts per million (ppm) and are referenced to the residual proton (4.70 ppm for D_2O and 7.26 ppm for $CDCl_3$) of the deuterated solvent. HPLC mass spectra were obtained on a Q-Tof premier-UPLC system equipped with an electrospray interface (ESI) (Waters, USA). Eluant A was composed of 95% (0.1% formic acid, 2 mM ammonium formate) and 5 % CH_3CN. Eluant B was composed of 5% (0.1% formic acid, 2 mM ammonium formate) and 95% acetonitrile. UPLC conditions utilized a BEH RPC18 2.1 × 150 mm column eluted with a 30% A, 70% B at 0.4 mL/min. Retention times for compounds **1** and **3** were 0.83 min and 3.56 min, respectively.

Gas chromatography mass spectra (GCMS) were performed on a Thermo Finnigan Trace DSQ GC-MS in CI mode with CH_4 as reagent gas. IR spectra were recorded on a Perkin-Elmer Spectrum GX FTIR spectrometer in KBr pellets. Radio-TLC were analyzed on Bioscan 200 imaging scanner (Bioscan Inc., USA).

The progress of reactions was monitored by TLC (SiO_2, Macherey-Nagel, USA) and visualized by UV light. Flash chromatography was carried out on SiO_2 (12–40 g) (Analogix, Varian, USA). Elemental analysis was performed by Galbraith Laboratories (TN, USA).

^{64}Cu was produced at the NIH by the irradiation of a thin layer of ^{64}Ni (Isoflex, USA) electroplated on a solid gold internal target plate of the CS-30 cyclotron utilizing the nuclear reaction ^{64}Ni(p,n)^{64}Cu and separated from the target material as [^{64}Cu]$CuCl_2$ by anion chromatography as previously described. [62]

2.2 Chemistry

2.2.1. 1-[4,8-Bis-(2,2,2-trifluoro-acetyl)-1,4,8,11-tetraaza-cyclotetradec-1-yl]-2,2,2-trifluoro-ethanone (2)—This reaction was done similarly to the known procedure. [63] Briefly, to a solution of cyclam (1.05 g, 5.2 mmol) and triethylamine (0.710 mL, 5.2 mmol) in methanol (5 mL), was added ethyl trifluoroacetate (1.86 mL, 15.6 mmol). The reaction was stirred under argon at room temperature (RT) for 5 h. The volatile solvents were removed in vacuo and the crude product was purified on a silica gel flash chromatography and eluted with 100% EtOAc. The eluent was evaporated to give **2** as white foam (2.2 g, 4.5 mmol, 86%). ^{1}H NMR (300 MHz, $CDCl_3$): δ 1.4–1.2 (m, 2H), 1.95–1.65 (m, 2H), 2.80–2.60 (m, 2H), 3.05–2.88 (m, 2H), 3.85–3.40 (m, 12H). GC-MS (CI-CH_4) 489 (M^+, 100%).

2.2.2. 1-(4,8-Bis-(2,2,2-trifluoro-acetyl)-11-{4-[4,8,11-tris-(2,2,2-trifluoro-acetyl)-1,4,8,11-tetraaza-cyclotetradec-1-ylmethyl]-benzyl}-1,4,8,11-tetraaza-cyclotetradec-1-yl)-2,2,2-trifluoro-ethanone (3)—This reaction was conducted as previously described. [40] To a solution of **2** (1.78 g, 3.64 mmol) in CH_3CN (20 mL) were added

α , α ′-dibromoxylene (0.481 g, 1.82 mmol) and K_2CO_3 (1.5 g, 10.9 mmol). The reaction was refluxed over night. After solvent evaporation, the crude product was extracted with CH_2Cl_2 and H_2O, dried over $MgSO_4$, evaporated and purified on silica gel flash chromatography using gradient of CH_2Cl_2/MeOH as eluent, to give **3** as a white solid in a yield of 66% (2.6 g, 2.41 mmol). ^{1}H NMR (300 MHz, $CDCl_3$): δ 1.86–1.65 (m, 4H), 2.56–2.01 (m, 8H), 2.80 (s, 4H), 3.78–3.34 (m, 28H), 7.15 (s, 4H). LC-MS: 1079 [M+H$^+$].

2.2.3 1,1′-{1,4-phenylenebis(methylene)}-bis{1,4,8,11-tetraaza-cyclotetradecane} –AMD3100 (1)—This reaction was conducted as described elsewhere. [64] In brief, to a solution of **3** (1.1 g, 1.02 mmol) in 5 mL of methanol were added K_2CO_3 (0.43 g, 3.1 mmol). The suspension was refluxed for 3 h. Then the reaction was cooled and toluene (10 mL) was added. The methanol was evaporated and $MgSO_4$ was added to the toluene suspension. The solution was filtered and toluene was concentrated to give **1** as a free base with a yield of 66% (0.34 g, 0.67 mmol).

^{1}H NMR (300 MHz, D_2O): δ 1.80–1.45 (m, 8H), 2.72–2.35 (m, 32H), 3.50 (s, 4H), 7.30 (s, 4H). LC-MS: 503 [M+H$^+$]. IR (KBr) ν (cm^{-1}) 553, 742, 768, 1076, 1218, 1478, 1587, 2662, 2962, 3411.

2.2.4 1, 1′-{1,4-phenylenebis(methylene)}-bis{1,4,8,11-tetraaza-cyclotetradecane}copper acetate (4)—This reaction was done similarly to the known procedure. [40] To a stirred solution of **1** (0.3 g, 0.6 mmol) in 5 mL methanol were added Cu(II) acetate (0.108 g, 0.6 mmol) in a solution of 0.4M NH_4OAc, pH = 5.5. The solution became blue-purple almost immediately. The mixture was stirred for 1 h and then triturated with diethyl ether to give **4** (0.2 g, 0.354 mmol) as a blue-purple precipitate, which was filtered and dried *in vacuo* to give 59% chemical yield.

^{1}H NMR (300 MHz, D_2O): δ 1.90 (CH_3CO_2H, s, 9H), 1.80–1.45 (m, 8H), 2.90–2.40 (m, 32H), 3.50 (s, 3H), 7.30 (s, 4H).

IR (KBr) ν (cm^{-1}) 518, 597, 721, 799, 835, 1131, 1204, 1429, 1474, 1677, 3438. Anal. Calcd for $C_{28}H_{51}N_8{\cdot}Cu{\cdot}(OAc)_3{\cdot}2H_2O$: C, 52.59%; H, 8.31%; N, 14.43%; Cu, 8.18%. Found: C, 52.70%; H, 7.94%; N, 14.38%; Cu, 6.21%.

2.3 Radiochemistry

2.3.1 [^{64}Cu]-1′-{1,4-phenylenebis(methylene)}-bis{1,4,8,11-tetraaza-cyclotetradecane}copper acetate (^{64}Cu-4)—^{64}Cu-chloride was converted to ^{64}Cu-acetate by adding 0.5 mL of 0.4 M NH_4OAc pH = 5.5 solution to 20 μL ^{64}Cu-chloride. ^{64}Cu-acetate solution (0.4 mL; 3.5–8 mCi, 130–296 MBq) was added into a solution of various amounts of **1** dissolved in 0.4 M NH_4OAc pH = 5.5 as indicated. The reaction was stirred for 1 h at RT. Thereafter, the radiochemical purity was determined using C-18 TLC plates (KC18F, 60 A, 200 μm, Whatman USA), developed in 2% ethylenediaminetetraacetic acid (EDTA) in water.

2.4 Biology

2.4.1 Animals—C57BL/6 mice were purchased from Taconic (Germantown, NY) and housed under specific pathogen free conditions. All animal studies were conducted in accordance with the principles and procedures outlined in the National Institute of Health Guide for the Care and Use of Animals on approved studies from the National Institutes of Health Institutional Animal Care and Use Committee.

2.4.2 Cells—Jurkat cells were purchased from the ATCC and grown in RPMI supplemented with 10% fetal bovine serum, 1 mM sodium pyruvate, 2 mM L-glutamine and Penicillin-Streptomycin (Gibco, CA).

A single cell suspension of mouse splenocytes was prepared by disrupting a spleen and lysing red cells using ACK solution (Quality Biological, MD).

2.4.3 Transwell migration assays—600 μL of migration medium (RPMI supplemented with 1% fetal bovine serum) containing SDF-1 (PeproTech, NJ), at the concentration indicated, were placed into the lower chamber of a Costar 24-well transwell (Corning, NY). 10^5 Jurkat cells in 100 μL migration medium were placed into the upper chamber (pore size 5 μm) and cells were collected from lower chamber after 3 h of migration at 37°C, and counted by flow cytometry using counting beads. Control migrations were performed without the chemokine in the lower chamber.

2.4.4 Binding assay—Cells (10^4 per well) were incubated with increasing concentrations of **4** and 250 nCi (9.25 KBq) of **^{64}Cu-4** for 1 h, after which cells were harvested onto a filter (Perkin-Elmer, USA) using Cell Harvester 96 (Tomtec, USA). Thereafter, scintillation fluid (Packard Bioscience, CT, USA) was added to the filter. Disintegrations were measured using a β^- counter (1450 Microbeta, Perkin-Elmer, USA).

2.4.5 Biodistribution—25 μCi (0.925 MBq, total mass ≤ 2 ng) of **^{64}Cu-4** in a volume of 100 μL were injected through the tail vein of C57BL/6 mice. One, two and 6 h post injection, blood was drawn from the heart under anesthesia and the mice were sacrificed. Spleen, liver, muscle, kidney, mesenteric lymph nodes (LN), intestine and femurs were removed. BM was flushed from within the bones, and the remaining organs were weighed. All organs were assayed for radioactivity using a gamma counter (1480 Wizard 3, Perkin-Elmer, USA). In blocking experiments, the tracer was injected together with 50 μg of **4**. Blocking experiments with SDF-1 were done by injecting the mice with 10 μg of the chemokine 20 min prior to- and together with the tracer (total of 20 μg per mouse). The results are presented as percent injected dose per gram tissue (%ID/g). Each group contained 5–6 mice.

2.4.6 PET studies—Mice (18 – 22 g) were anesthetized using isoflurane/O_2 (1.5–5% v/v) and injected with 25–26 μCi (0.925–0.962 MBq, total mass ≤ 2 ng) of **^{64}Cu-4** or free ^{64}Cu-acetate via the tail vein in a total volume of 100 μL PBS. For blocking experiments, the tracer was injected together with 50 μg of **4**. PET scans were performed using the Advanced Technology Laboratory Animal Scanner (ATLAS) PET scanner. [65] Whole-body (40, 80 and 120 min; five bed positions, each 8 min) scans were started approximately two min after radiotracer injection and recorded with a 100–700 keV energy window. Each group consisted of at least five mice. The images were reconstructed by a two-dimensional ordered subsets expectation maximum (2D-OSEM) algorithm, and no correction was applied for attenuation or scatter. Image analysis was done using ImageJ version 1.4g (NIH, USA) and OsiriX version 2.7.5 (Switzerland) software. The results were calculated as percentage injected dose per gram (%ID/g). At the end of each experiment a ^{64}Cu source of known activity was imaged to obtain KBq of ^{64}Cu per counts per seconds for the imaging system (calibration factor). Then, every ROI (counts per second per cubic centimeter) was multiplied by this factor and divided by injected activity.

2.4.7 Flow cytometry—Jurkat cells (10^6 in 100 μL of PBS supplemented with 4% FBS) were blocked with serum for five min on ice and then stained with PE-conjugated anti-human CXCR4 or isotype control (R&D Systems, MN). Cells were acquired on an LSRII (BectonDickinson, CA) and analyzed using FlowJO (Tree Star, OR).

Results and Discussion

1 is a symmetrical bicyclam that is a highly specific CXCR4 antagonist and that can bind to metal ions such as Cu(II) [66]. It was demonstrated that a complex between **1** and metal ions such as Ni(II), Zn(II) and Cu(II) improved the interaction of the cyclam complex with a carboxylate group of an aspartate residue within the binding pocket of CXCR4. [66] There are several synthetic routes to obtain **1** which involves optimization of reaction conditions such as pH, [67] temperature, and concentration [63]. Other methods involve blocking of amino groups using phosphorus [68, 69] or metal-tricarbonyl, [70] but involve the use of anhydrous material and undesirable solvents. In addition, a direct synthetic route for **1** without the need of protecting groups, [71] requires more synthetic steps and no improvement of the yield.

The synthesis of **1**, as a free base, included three steps (Fig. 2); (i) protecting on the cyclam (ii) bis-alkylation - dimerization and (iii) deprotection. [63, 40] The protection of the amine on the cyclam ring was done similarly to the procedure of Yang et. al., [63, 72] using four equivalents of ethyl trifluororacetate (EtOTFA) as a selective acetylation agent. However, we obtained a mixture of 60% fully protected cyclam and only 40% of the desired product, **2**, which contains one free amine as established by GCMS and NMR. Hence, we modified the synthesis and used only three equivalent of EtOTFA under the same reaction conditions as described in the experimental section, and we succeeded in obtaining **2** with a conversion > 99% and 86% yield. The dimerization of two cyclam rings and the de-protection of the TFA groups to furnish **1** as a free base were done as previously published. [40, 64]

1 was used for the preparation of cold standard, **4,** containing Cu(II) ion (Fig. 3), and as a precursor for the radiosynthesis with ^{64}Cu (Fig. 3). The incorporation of a single Cu(II) ion into **1** was assured by using 1 equivalent of $Cu(OAc)_2$. The incorporation reaction was conducted in methanol; however, in order to obtain better solubility, $Cu(OAc)_2$ was first dissolved in a small volume of NH_4OAc buffer (0.1–0.2 mL). The incorporation was verified using IR and elemental analysis.

The incorporation reaction was optimized for the smallest amount of substrate because we wished to avoid the need to remove excess unlabeled ligand **(1)**. Increasing amounts of **1** were added to aqueous [^{64}Cu]-$Cu(OAc)_2$ solution at pH 5.5 and incubated for 1 h at RT. The percent of incorporation was monitored by radio TLC. At substrate masses less than 0.4 μg of **1**, two peaks were observed by radio TLC (R_f ~ 0.1, **^{64}Cu-4;** R_f ~ 0.6 free ^{64}Cu). At mass greater than or equal to 0.4 μg, only the desired product, **^{64}Cu-4** was observed as a single peak. The absence of free ^{64}Cu-acetate at R_f ~ 0.6 indicated that the formation of complex **^{64}Cu-4** was completed. The lowest amount of **1** needed for 100 % incorporation was determined as 0.4 μg (Fig 4) providing a highest specific activity (SA) of 11,280 Ci/mmol ($4.17 \cdot 10^5$ GBq/mmol) at the end of radiosynthesis (n=10). The ability to obtain 100% complex formation has been shown previously by McCarthy et al. for the incorporation of ^{64}Cu into a TETA chelator. [52]

Gerlach et al. demonstrated that incorporation of metal ions into **1** improved the binding affinity towards CXCR4, as measured by inhibiting binding of SDF-1 and anti-CXCR4 antibody. [66] In order to verify that incorporation of Cu(II) ion enhances the binding of **1** to CXCR4, we evaluated binding in Jurkat T cells. We established that the Jurkat T-cells express high levels of CXCR4 using flow cytometry (Fig. 5a). The cells were then incubated with a constant amount of **^{64}Cu-4** and increasing concentrations of non-radioactive **4** for 1 h at RT (Fig 5b). The IC_{50} of **^{64}Cu-4** binding to Jurkat cells was 62.7 μM. In order to evaluate the binding of **^{64}Cu-4** to mouse cells we repeated the experiment with mouse splenocytes, and obtained a similar IC_{50} of 46.9 μM (Fig. 5c). This is the first published result of homologous displacements for **1**. Heterologous displacement of radiolabeled antibody with **4** showed lower IC_{50} of 0.1

μM by Gerlach et al., [66] and an IC_{50} of 15.2 μM was reported by Gupta et al., which was done by competition of **1** with ^{125}I-SDF-1 using HL-60 cells. [73]

In order to verify that the CXCR4 inhibitory characteristics of **4** are not affected by the incorporation of Cu(II) ion, we evaluated the ability of **^{64}Cu-4** to inhibit Jurkat cells migration towards SDF-1. Migration was tested through 5 μm pore membrane in a standard assay format. We used SDF-1 in the lower wells at 100 ng/mL, the lowest concentration that induces maximal migration, and tested various concentrations of **4** and **1** in the upper wells. Both **1** and **4** were found to inhibit Jurkat migration to SDF-1 in a similar manner with IC_{50}'s of 27.4 nM and 75.4 nM, respectively (Fig 6). This result indicates that **4** retain the ability to inhibit SDF-1-induced chemotaxis through CXCR4. A comparison between the binding affinity of **4** towards CXCR4, versus its migration inhibition, revealed a 1000 fold discrepancy between the binding as measured by homologous displacement and functional activity. A similar discrepancy has been observed between activity of AMD3100 and heterologous displacement of SDF-1. [66] Another interesting observation was reported for a different chemokine receptor, CCR1. Jensen et al. showed that a low affinity small molecule agonist can act as an allosteric enhancer for CCL3 and at the same time as a competitive blocker of the binding of CCL5 through binding deep in the main ligand binding pocket. [74] Although we cannot explain these discrepancies, we postulate that AMD3100 may show high-affinity interactions to the SDF-1-bound form of CXCR4 (positive co-operativity), producing a non-signaling conformation.

The biodistribution of **^{64}Cu-4** was analyzed in immune competent C57BL/6 mice using both PET scans in live animals and organ dissection and gamma counting. Since multiple immune cells express CXCR4, we would expect the tracer to accumulate in immune-related organs such as the spleen, lymph nodes and bone marrow. Mice were divided into six groups: three groups were injected (i.v.) only with **^{64}Cu-4** and sacrificed after 1, 2 and 6 h. A forth and fifth groups were designed to test the specific binding of **4** *in vivo* and was co-injected with excess of cold tracer and sacrificed 2 or 6 h post injection. The sixth group was injected with SDF-1 to evaluate specific binding of **^{64}Cu-4** to CXCR4, and sacrificed after 2 h. Spleen, intestine, LN, femoral BM, blood, liver, muscle and kidney were removed for gamma-counting (Fig 7).

Uptake of **^{64}Cu-4,** measured by percent ID/g of tissue**,** was detected after 1 h in the liver (41%) and kidneys (10%). High accumulation of **^{64}Cu-4** was also observed in immune related organs; spleen (13%), BM (14%) and LN (10%). **^{64}Cu-4** uptake was low in blood and muscle (1.7% and 0.3%, respectively). 2 h-post injection there were significant changes in **^{64}Cu-4** accumulation only in the blood which was reduced to <1%, and a slight increase in the liver to 49% (Fig 7a). A slight increase of **^{64}Cu-4** was observed in the spleen, LN, liver and BM 6 h post injection (Fig 7a). Co-injection of excess of non-labeled **4** resulted in reduced accumulation of **^{64}Cu-4** in all immune related organs by 60–80 % in comparison to the accumulation after 2 or 6 h (Figs 7b, 7c). Surprisingly, the accumulation of **^{64}Cu-4** in the liver was also reduced by 79% and 74% after 2 and 6 h respectively, which suggests specific binding of **4** in the liver. There was a corresponding increase in accumulation of **^{64}Cu-4** in the kidneys, presumably due to a reduction in specific binding and enhanced renal clearance. [75] Injection of 10 μg SDF-1 20 min prior to and together with the **^{64}Cu-4** reduced the accumulation of **^{64}Cu-4** in the liver, BM and slightly in the spleen (Fig. 7b). The lower reduction of the tracer accumulation after excess of SDF-1 injection in comparison to excess of **4** could be due to differences in distribution and/or pharmaco-kinetics of the SDF-1 protein vs. the small molecule AMD3100. In addition, the possible binding of SDF-1 to glycosaminoglycans and heparin sulphate *in-vivo* might reduce the bioavailability of SDF-1 to bind CXCR4. [76] CXCR4 expression in the liver is reportedly limited to sinusoidal endothelial cells[77], oval cells, [78, 79] and to immune cells, [80] which are unlikely to account for the high hepatic accumulation of **^{64}Cu-4** – although inhibition of liver binding by SDF-1 indicates a CXCR4-dpendent component. It is possible that hepatocytes or other liver cells take up **^{64}Cu-4** through CXCR4-

independent pathways, which are blocked by excess cold **4,** but not by SDF-1. In accordance, Misra et al. found that ^{99}Tc labeled SDF-1 did not accumulate in the liver. [61] Hence, the specificity of **1** for CXCR4 should be re-examined in binding assays using liver membrane preparations.

The differences between our biodistribution results and other reported biodistribution of labeled CXCR4 ligands SDF-1 [61] and Ac-TZ14011, [60] might be explained by the different pharmaco-kinetics of small protein and small peptide respectively, and the pharmaco-kinetics of a small molecule such as AMD3100.

In addition to biodistribution experiments, mice were also scanned with ATLAS, to visualize the uptake in the various organs. The rapid renal clearance of **^{64}Cu-4** resulted in high accumulation of **^{64}Cu-4** in the bladder within 2 h (Fig. 8b). As was revealed by organ analyses, there was high accumulation of **^{64}Cu-4** in the liver, kidney and spleen. Blocking with excess of non-radioactive **4** reduced the uptake in the spleen and liver to undetectable levels, and increased the accumulation in the kidneys, in accordance with the biodistribution results (Figs. 8a and 8b). In addition, to verify that the activity was due to accumulation of **^{64}Cu-4** rather than free ^{64}Cu, mice were scanned after injection of free ^{64}Cu. The uptake of the free isotope was in the liver and intestine (Figs. 8a and 8b). There was no uptake in the spleen, and low accumulation in the bladder. These results indicate that free ^{64}Cu does not accumulate in immune organs.

Biodistribution and PET scans revealed that **^{64}Cu-4** accumulates mainly in organs known to contain high densities of CXCR4-expressing cells, as well as liver and kidney. The accumulation of **^{64}Cu-4** in CXCR4 expressing tissues, along with evidence of specific competition in vivo by SDF-1, support further evaluation of **^{64}Cu-4** as a potential marker for the imaging of CXCR4 in tissues such as tumors.

Conclusions

We prepared **^{64}Cu-4,** a potent CXCR4 antagonist, in high radiochemical yield and with high radiochemical purity. **^{64}Cu-4** was as potent as **1** in inhibiting the activity of CXCR4. Thus, we expected no alteration in *in vivo* characteristics of **^{64}Cu-4** vs. **1**, including binding to CXCR4 and acting as a CXCR4 antagonist. Biodistribution studies revealed uptake by organs and tissues involved in the immune system of mice as well as in the liver. Uptake in the liver, which although specific, may have a CXCR4-independent component and may detract from the usefulness of this radiotracer for imaging cancers in the liver. We conclude that **^{64}Cu-4** might be useful for discriminating CXCR4 positive and negative tumors, and for directing the use and monitoring the effectiveness of CXCR4-targeted therapies.

Acknowledgments

This research was supported by Intramural Research Programs of the National Institute of Biomedical Imaging and Bioengineering (NIBIB) and the National Institute of Allergy and Infectious Diseases (NIAID). We would like to thank Dr. Amnon Peled from Hadassah-Hebrew University Medical Center, Jerusalem, Israel, for fruitful discussions and Dr. Ying Ma for HPLC-MS analysis.

References

1. Zlotnik A. J Pathol 2008;215:211. [PubMed: 18523970]
2. Zlotnik A, Yoshie O. Immunity 2000;12:121. [PubMed: 10714678]
3. Scotton CJ, Wilson JL, Scott K, Stamp G, Wilbanks GD, Fricker S, Bridger G, Balkwill FR. Cancer Res 2002;62:5930. [PubMed: 12384559]

4. Zimmerman NP, Vongsa RA, Wendt MK, Dwinell MB. Inflamm Bowel Dis 2008;14:1000. [PubMed: 18452220]
5. Rollins BJ. Blood 1997;90:909. [PubMed: 9242519]
6. Murphy PM. Methods Mol Biol 2000;138:89. [PubMed: 10840745]
7. Rossi D, Zlotnik A. Annu Rev Immunol 2000;18:217. [PubMed: 10837058]
8. Balkwill F, Mantovani A. Lancet 2001;357:539. [PubMed: 11229684]
9. Vicari AP, Caux C. Cytokine Growth Factor Rev 2002;13:143. [PubMed: 11900990]
10. Schols D. Antiviral Res 2006;71:216. [PubMed: 16753228]
11. Horuk R. Cytokine Growth Factor Rev 2001;12:313. [PubMed: 11544102]
12. Phillips RJ, Burdick MD, Lutz M, Belperio JA, Keane MP, Strieter RM. Am J Respir Crit Care Med 2003;167:1676. [PubMed: 12626353]
13. Bleul CC, Wu L, Hoxie JA, Springer TA, Mackay CR. Proc Natl Acad Sci U S A 1997;94:1925. [PubMed: 9050881]
14. Gupta SK, Lysko PG, Pillarisetti K, Ohlstein E, Stadel JM. J Biol Chem 1998;273:4282. [PubMed: 9461627]
15. Hesselgesser J, Halks-Miller M, DelVecchio V, Peiper SC, Hoxie J, Kolson DL, Taub D, Horuk R. Curr Biol 1997;7:112. [PubMed: 9024623]
16. Patrussi L, Baldari CT. Immunol Lett 2008;115:75. [PubMed: 18054087]
17. Chen WJ, Jayawickreme C, Watson C, Wolfe L, Holmes W, Ferris R, Armour S, Dallas W, Chen G, Boone L, Luther M, Kenakin T. Mol Pharmacol 1998;53:177. [PubMed: 9463473]
18. Li JK, Yu L, Shen Y, Zhou LS, Wang YC, Zhang JH. World J Gastroenterol 2008;14:2308. [PubMed: 18416455]
19. Yoon Y, Liang Z, Zhang X, Choe M, Zhu A, Cho HT, Shin DM, Goodman MM, Chen ZG, Shim H. Cancer Res 2007;67:7518. [PubMed: 17671223]
20. Libura J, Drukala J, Majka M, Tomescu O, Navenot JM, Kucia M, Marquez L, Peiper SC, Barr FG, Janowska-Wieczorek A, Ratajczak MZ. Blood 2002;100:2597. [PubMed: 12239174]
21. Redjal N, Chan JA, Segal RA, Kung AL. Clin Cancer Res 2006;12:6765. [PubMed: 17121897]
22. Balkwill F. Semin Cancer Biol 2004;14:171. [PubMed: 15246052]
23. Tanaka T, Bai Z, Srinoulprasert Y, Yang BG, Hayasaka H, Miyasaka M. Cancer Sci 2005;96:317. [PubMed: 15958053]
24. Ma Q, Jones D, Borghesani PR, Segal RA, Nagasawa T, Kishimoto T, Bronson RT, Springer TA. Proc Natl Acad Sci U S A 1998;95:9448. [PubMed: 9689100]
25. Nagasawa T, Tachibana K, Kishimoto T. Semin Immunol 1998;10:179. [PubMed: 9653044]
26. Zou YR, Kottmann AH, Kuroda M, Taniuchi I, Littman DR. Nature 1998;393:595. [PubMed: 9634238]
27. Burger JA, Burkle A. Br J Haematol 2007;137:288. [PubMed: 17456052]
28. Barbero S, Bonavia R, Bajetto A, Porcile C, Pirani P, Ravetti JL, Zona GL, Spaziante R, Florio T, Schettini G. Cancer Res 2003;63:1969. [PubMed: 12702590]
29. Muller A, Homey B, Soto H, Ge N, Catron D, Buchanan ME, McClanahan T, Murphy E, Yuan W, Wagner SN, Barrera JL, Mohar A, Verastegui E, Zlotnik A. Nature 2001;410:50. [PubMed: 11242036]
30. Murphy PM. N Engl J Med 2001;345:833. [PubMed: 11556308]
31. Tamamura H, Hori A, Kanzaki N, Hiramatsu K, Mizumoto M, Nakashima H, Yamamoto N, Otaka A, Fujii N. FEBS Lett 2003;550:79. [PubMed: 12935890]
32. Taichman RS, Cooper C, Keller ET, Pienta KJ, Taichman NS, McCauley LK. Cancer Res 2002;62:1832. [PubMed: 11912162]
33. Rubin JB, Kung AL, Klein RS, Chan JA, Sun Y, Schmidt K, Kieran MW, Luster AD, Segal RA. Proc Natl Acad Sci U S A 2003;100:13513. [PubMed: 14595012]
34. Marchesi F, Monti P, Leone BE, Zerbi A, Vecchi A, Piemonti L, Mantovani A, Allavena P. Cancer Res 2004;64:8420. [PubMed: 15548713]
35. Darash-Yahana M, Pikarsky E, Abramovitch R, Zeira E, Pal B, Karplus R, Beider K, Avniel S, Kasem S, Galun E, Peled A. Faseb J 2004;18:1240. [PubMed: 15180966]

36. Sun YX, Schneider A, Jung Y, Wang J, Dai J, Cook K, Osman NI, Koh-Paige AJ, Shim H, Pienta KJ, Keller ET, McCauley LK, Taichman RS. J Bone Miner Res 2005;20:318. [PubMed: 15647826]
37. Xia MQ, Hyman BT. J Neurovirol 1999;5:32. [PubMed: 10190688]
38. Bezzi P, Domercq M, Brambilla L, Galli R, Schols D, De Clercq E, Vescovi A, Bagetta G, Kollias G, Meldolesi J, Volterra A. Nat Neurosci 2001;4:702. [PubMed: 11426226]
39. Rauer M, Pagenstecher A, Schulte-Monting J, Sauder C. J Neurovirol 2002;8:168. [PubMed: 12053272]
40. Bridger GJ, Skerlj RT, Thornton D, Padmanabhan S, Martellucci SA, Henson GW, Abrams MJ, Yamamoto N, De Vreese K, Pauwels R, et al. J Med Chem 1995;38:366. [PubMed: 7830280]
41. Bridger GJ, Skerlj RT, Padmanabhan S, Martellucci SA, Henson GW, Struyf S, Witvrouw M, Schols D, De Clercq E. J Med Chem 1999;42:3971. [PubMed: 10508445]
42. De Clercq E, Yamamoto N, Pauwels R, Balzarini J, Witvrouw M, De Vreese K, Debyser Z, Rosenwirth B, Peichl P, Datema R, et al. Antimicrob Agents Chemother 1994;38:668. [PubMed: 7913308]
43. Joao HC, De Vreese K, Pauwels R, De Clercq E, Henson GW, Bridger GJ. J Med Chem 1995;38:3865. [PubMed: 7562918]
44. Rosenkilde MM, Gerlach LO, Hatse S, Skerlj RT, Schols D, Bridger GJ, Schwartz TW. J Biol Chem 2007;282:27354. [PubMed: 17599916]
45. Fricker SP, Anastassov V, Cox J, Darkes MC, Grujic O, Idzan SR, Labrecque J, Lau G, Mosi RM, Nelson KL, Qin L, Santucci Z, Wong RS. Biochem Pharmacol 2006;72:588. [PubMed: 16815309]
46. Hu JS, Freeman CM, Stolberg VR, Chiu BC, Bridger GJ, Fricker SP, Lukacs NW, Chensue SW. Am J Pathol 2006;169:424. [PubMed: 16877345]
47. Khan A, Greenman J, Archibald SJ. Curr Med Chem 2007;14:2257. [PubMed: 17896975]
48. Schols D, Struyf S, Van Damme J, Este JA, Henson G, De Clercq E. J Exp Med 1997;186:1383. [PubMed: 9334378]
49. Mishani E, Abourbeh G. Curr Top Med Chem 2007;7:1755. [PubMed: 17979785]
50. Elsinga PH. Methods 2002;27:208. [PubMed: 12183108]
51. Shiue CY, Welch MJ. Radiol Clin North Am 2004;42:1033. [PubMed: 15488556]
52. McCarthy DW, Shefer RE, Klinkowstein RE, Bass LA, Margeneau WH, Cutler CS, Anderson CJ, Welch MJ. Nucl Med Biol 1997;24:35. [PubMed: 9080473]
53. Jones-Wilson TM, Deal KA, Anderson CJ, McCarthy DW, Kovacs Z, Motekaitis RJ, Sherry AD, Martell AE, Welch MJ. Nucl Med Biol 1998;25:523. [PubMed: 9751418]
54. Lewis JS, Connett JM, Garbow JR, Buettner TL, Fujibayashi Y, Fleshman JW, Welch MJ. Cancer Res 2002;62:445. [PubMed: 11809694]
55. Sun X, Wuest M, Weisman GR, Wong EH, Reed DP, Boswell CA, Motekaitis R, Martell AE, Welch MJ, Anderson CJ. J Med Chem 2002;45:469. [PubMed: 11784151]
56. Sun X, Wuest M, Kovacs Z, Sherry AD, Motekaitis R, Wang Z, Martell AE, Welch MJ, Anderson CJ. J Biol Inorg Chem 2003;8:217. [PubMed: 12459917]
57. Anderson CJ, Wadas TJ, Wong EH, Weisman GR. Q J Nucl Med Mol Imaging 2008;52:185. [PubMed: 18043536]
58. Sun X, Kim J, Martell AE, Welch MJ, Anderson CJ. Nucl Med Biol 2004;31:1051. [PubMed: 15607487]
59. Wu AM, Yazaki PJ, Tsai S, Nguyen K, Anderson AL, McCarthy DW, Welch MJ, Shively JE, Williams LE, Raubitschek AA, Wong JY, Toyokuni T, Phelps ME, Gambhir SS. Proc Natl Acad Sci U S A 2000;97:8495. [PubMed: 10880576]
60. Hanaoka H, Mukai T, Tamamura H, Mori T, Ishino S, Ogawa K, Iida Y, Doi R, Fujii N, Saji H. Nucl Med Biol 2006;33:489. [PubMed: 16720240]
61. Misra P, Lebeche D, Ly H, Schwarzkopf M, Diaz G, Hajjar RJ, Schecter AD, Frangioni JV. J Nucl Med 2008;49:963. [PubMed: 18483105]
62. Szajek LP, Meyer W, Plascjak P, Eckelman WC. Radiochem Acta 2005;93:1.
63. Wen Y, Giandomenico CM, Sartori M, Moore DA. Tetrahedron letters 2003;44:2481.
64. 6489472, U. P. 2002.

65. Seidel J, Vaquero J, Green M. IEEE Trans Nucl Sci 2003;50:1347.
66. Gerlach LO, Jakobsen JS, Jensen KP, Rosenkilde MR, Skerlj RT, Ryde U, Bridger GJ, Schwartz TW. Biochemistry 2003;42:710. [PubMed: 12534283]
67. Zoltan Kovacs ADS. Synthesis 1997:759.
68. Gardinier I, Oget ARN, Bernard H, Yaouanc JJ, Handel H. Tetrahedron letters 1996;37:7711.
69. Marshall, DGaGR. Synthetic communications 1998;28:2903.
70. Patinec V, Clement JJYJC, Handel H, des Abbayes H. Tetrahedron letters 1995;36:79.
71. Achmatowicz M, Hegedus LS. J Org Chem 2003;68:6435. [PubMed: 12895083]
72. Xu D, Mattner PG, Prasad K, Repic O, Blacklock TJ. Tetrahedron letters 1996;37:5301.
73. Gupta SK, Pillarisetti K, Thomas RA, Aiyar N. Immunol Lett 2001;78:29. [PubMed: 11470148]
74. Jensen PC, Thiele S, Ulven T, Schwartz TW, Rosenkilde MM. J Biol Chem 2008;283:23121. [PubMed: 18559339]
75. Hendrix CW, Flexner C, MacFarland RT, Giandomenico C, Fuchs EJ, Redpath E, Bridger G, Henson GW. Antimicrob Agents Chemother 2000;44:1667. [PubMed: 10817726]
76. Laguri C, Arenzana-Seisdedos F, Lortat-Jacob H. Carbohydr Res 2008;343:2018. [PubMed: 18334249]
77. Li W, Gomez E, Zhang Z. J Exp Clin Cancer Res 2007;26:527. [PubMed: 18365549]
78. Mavier P, Martin N, Couchie D, Preaux AM, Laperche Y, Zafrani ES. Am J Pathol 2004;165:1969. [PubMed: 15579440]
79. Hatch HM, Zheng D, Jorgensen ML, Petersen BE. Cloning Stem Cells 002;4:339. [PubMed: 12626097]
80. Wald O, Weiss ID, Galun E, Peled A. Cytokine 2007;39:50. [PubMed: 17629707]

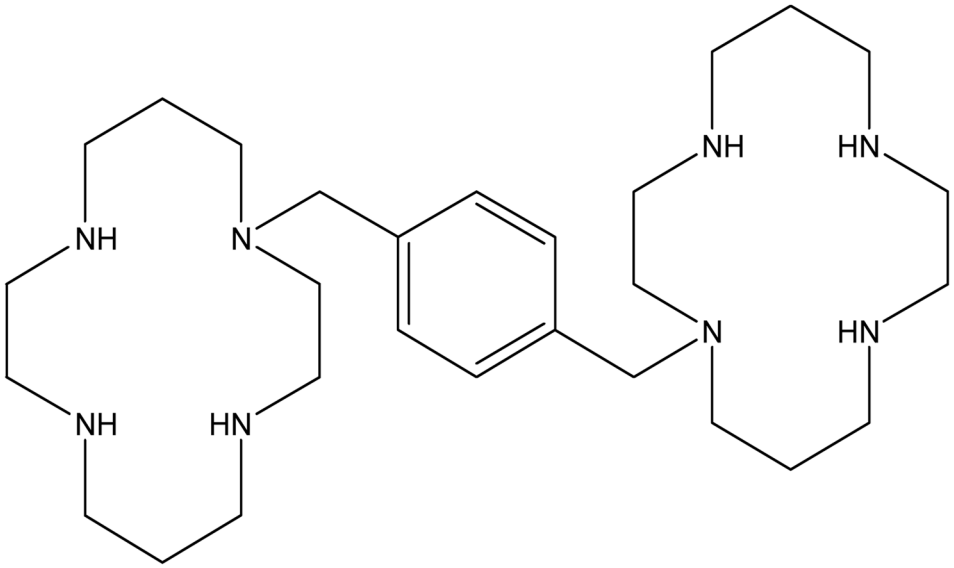

1 (AMD3100)

Figure 1.
Structure of AMD3100 (**1**).

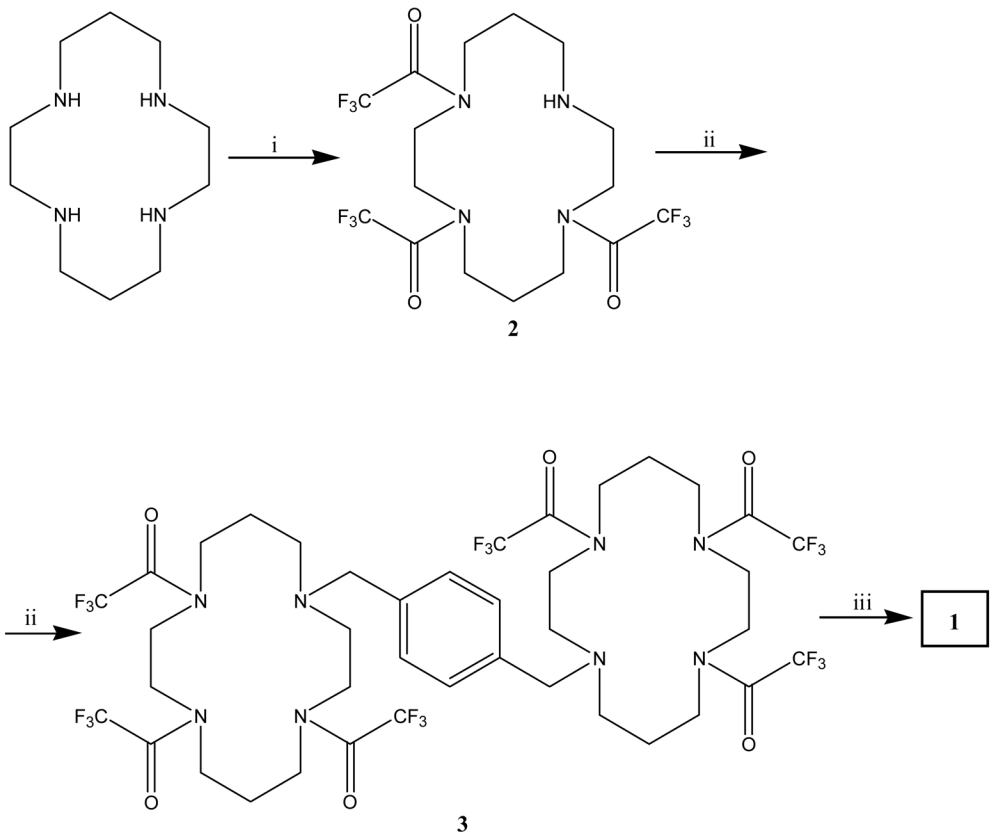

Figure 2.

Synthesis of **1**. Reagents and conditions: (i) ethyl trifluoroacetate, triethylamine, methanol 5 h, RT; (ii) α , α –dibromoxylene, K_2CO_3, CH_3CN, reflux, over-night; (iii) K_2CO_3, methanol, reflux 3 h.

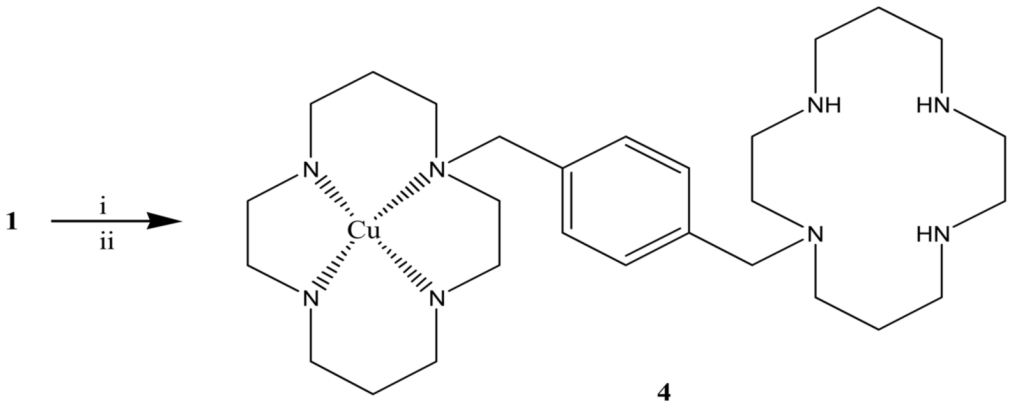

Figure 3.
Synthesis of **4**. Reagents and conditions: (i) Non-radioactive synthesis: Cu(II)acetate, methanol, NH_4- acetate, 1 h, RT; (ii) Radioactive synthesis: ^{64}Cu-Acetate, 1h, RT.

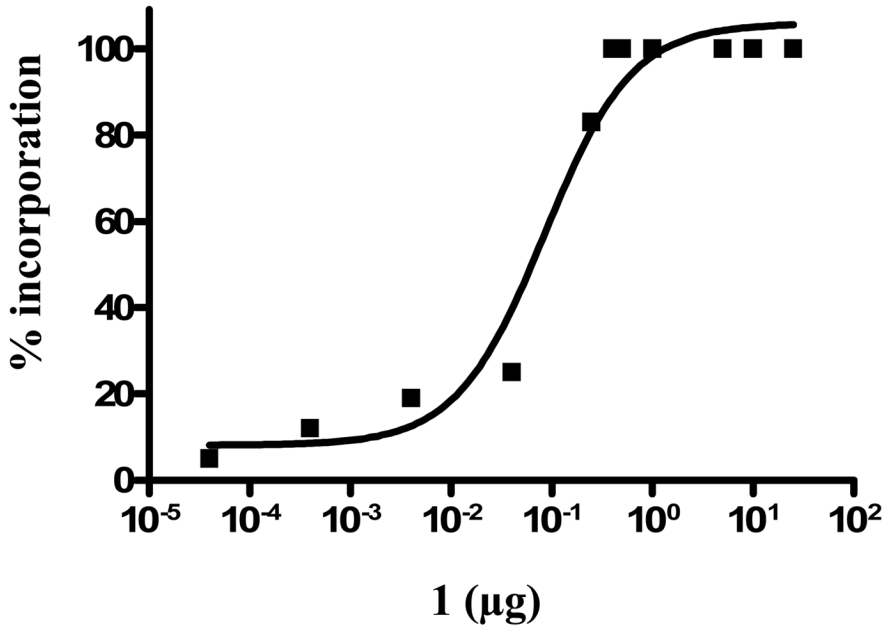

Figure 4.
Percent incorporation of ^{64}Cu into **1**

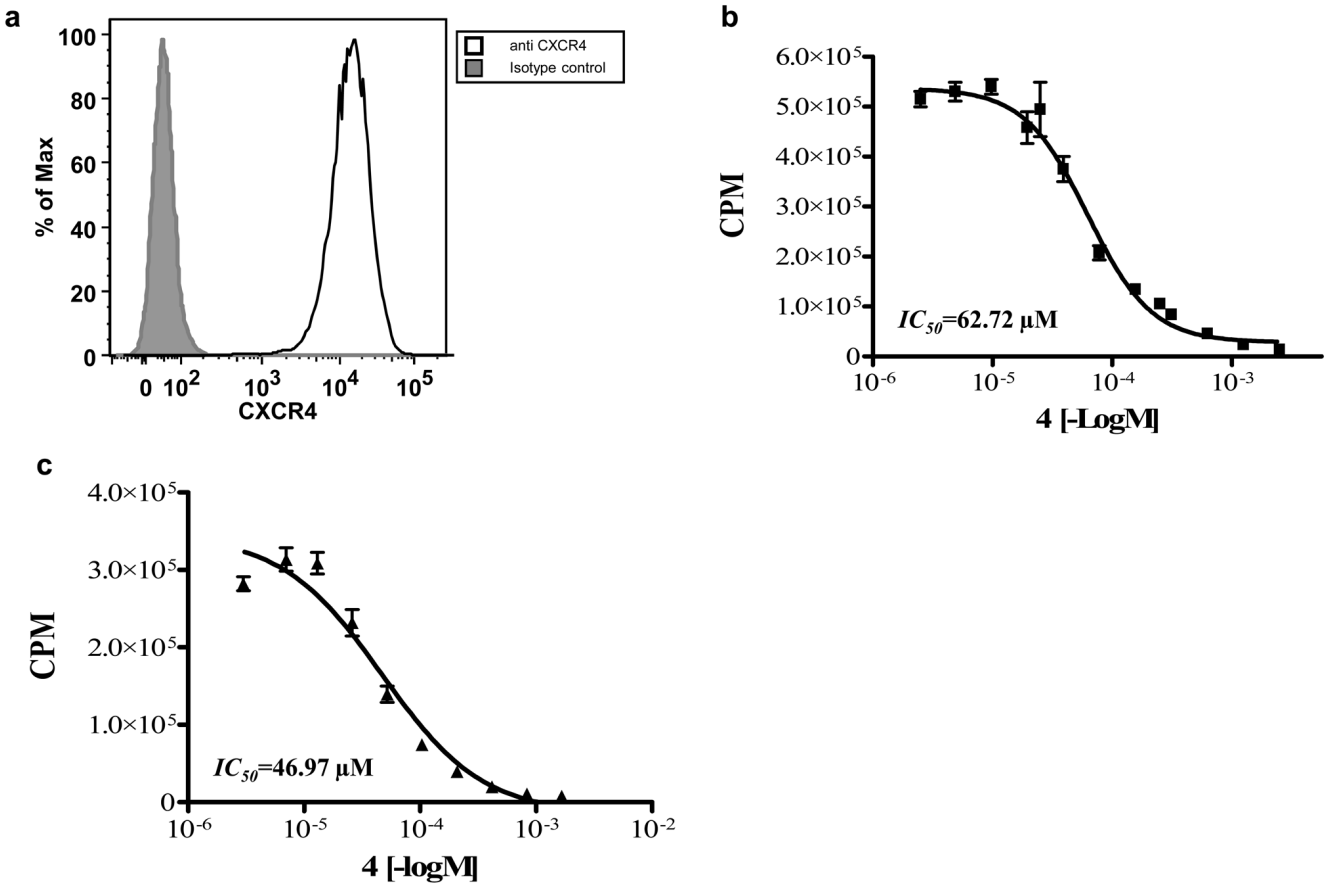

Figure 5.

(a) CXCR4 expression by Jurkat cells evaluated by flow cytometry. Gray histogram represents isotype control staining, black line represents anti CXCR4 staining (b) binding assay of **4** using Jurkat cell line (c) binding assay of **4** using mouse splenocytes. Results shown are average of three experiments.

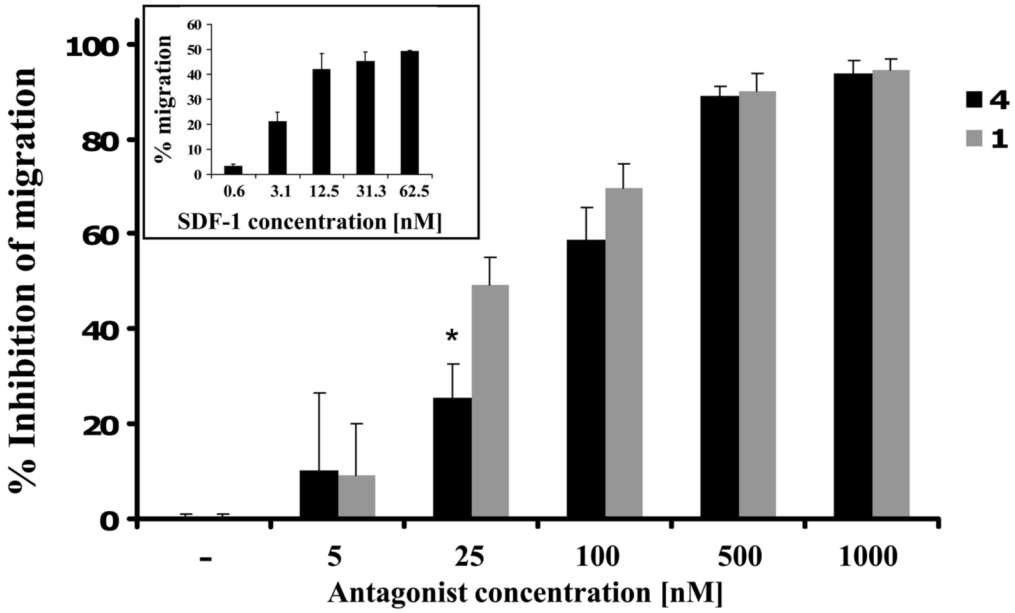

Figure 6.

Inhibition of SDF-1 induced migration of Jurkat cells by **1** and **4**. The lowest concentration of SDF-1 to induce maximal migration was 31.3 nM and was used in the inhibition experiments (small box). Results shown are average of 3 experiments ± SE. * $P<0.05$ calculated by Students two-tailed t-test comparing inhibition by **1** and **4**.

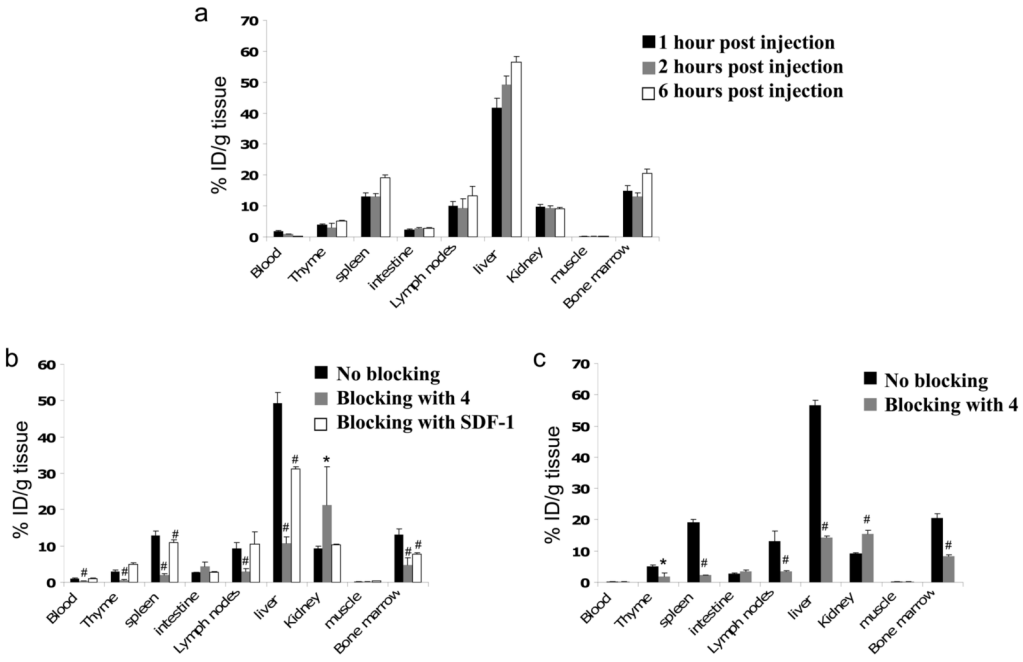

Figure 7.

(a) Biodistribution of ^{64}**Cu-4** in normal C57Bl/6 mice. (b) Blocking of ^{64}**Cu-4** accumulation 2 h after co-injection with 50 μg of **4** or 20 μg of SDF-1. (c) Blocking of ^{64}**Cu-4** accumulation 6 h after co-injection with 50 μg of **4.** Each group contains at least 5 mice. Results shown are average ± SE. * $P<0.05$, # $P<0.01$ calculated by Students two-tailed t-test comparing blocking with **4** or SDF-1 groups to 2 h or 6 h control group.

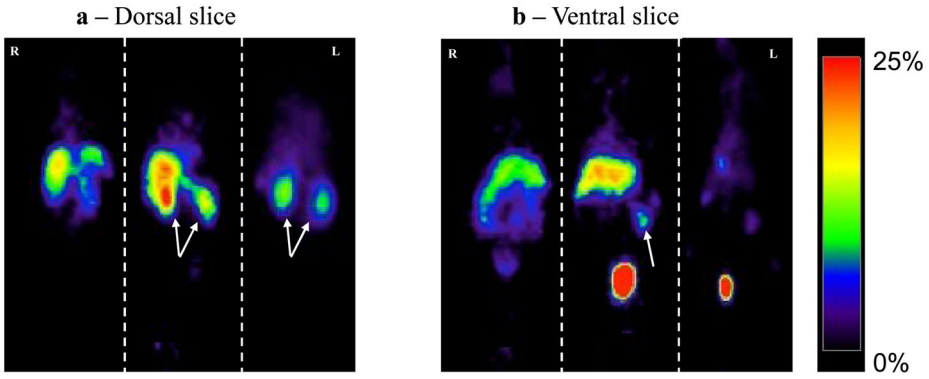

Figure 8.

Representative PET images (%ID/g) of C57Bl/6 mice 2 h after injection with 26 μCi of free **^{64}Cu** (left), **^{64}Cu-4** (middle) or co-injection of **^{64}Cu-4** and 50 μg of **4** (right). (a) Dorsal slice. Arrows indicate the kidneys. (b) Ventral slice. Arrow indicates the spleen.